

Topological Edge Floppy Modes in Disordered Fiber Networks

Di Zhou, Leyou Zhang, and Xiaoming Mao

Department of Physics, University of Michigan, Ann Arbor, Michigan 48109-1040, USA



(Received 12 August 2017; published 8 February 2018)

Disordered fiber networks are ubiquitous in a broad range of natural (e.g., cytoskeleton) and manmade (e.g., aerogels) materials. In this Letter, we discuss the emergence of topological floppy edge modes in two-dimensional fiber networks as a result of deformation or active driving. It is known that a network of straight fibers exhibits bulk floppy modes which only bend the fibers without stretching them. We find that, interestingly, with a perturbation in geometry, these bulk modes evolve into edge modes. We introduce a topological index for these edge modes and discuss their implications in biology.

DOI: [10.1103/PhysRevLett.120.068003](https://doi.org/10.1103/PhysRevLett.120.068003)

Introduction.—Recent theoretical advances in applying concepts of topological states of matter to mechanical systems have led to the burgeoning new field of “topological mechanics,” where nontrivial topologies of the phonon bands give rise to exotic mechanical and acoustic properties [1–20].

Among many different types of topological mechanical systems, a particularly interesting class consists of “Maxwell lattices,” which are central-force lattices with average coordination number $\langle z \rangle = 2d$, where d is the spatial dimension, and are thus on the verge of mechanical instability [2,3,16–20]. Maxwell lattices host topologically protected phonon edge modes at zero frequency (floppy modes). These edge modes are governed by the topology of the equilibrium and compatibility matrices of the lattice, which in turn are governed by the lattice geometry [2]. A simple two-dimensional (2D) example of Maxwell lattice, the deformed kagome lattice, as shown in Fig. 1, exhibits different phases where the topological structure changes and the floppy modes localize at different edges [17]. In particular, what drives the topological transition here is a soft strain that changes the lattice geometry, where all bonds remain the same length and only the bond angles change. At the topological transition, bonds form straight lines and floppy modes penetrate infinitely deep into the bulk, whereas in the two phases below and above the transition, the floppy modes localize at opposite edges. In the topologically nontrivial phase all floppy modes localize on the top edge, leaving the bottom edge rigid. This physics of the Maxwell lattices makes them both an interesting topic for theoretical study [21–27] and good candidates for the design of novel mechanical metamaterials where the edges can change stiffness by orders of magnitude reversibly [17].

Most existing studies of topological mechanics are based on periodic lattices, with only few exceptions [28,29]. In general, topological order is robust against disorder, because topological attributes are integer valued and remain invariant upon the addition of disorder until they jump to a

different integer value. This robustness has been demonstrated in various periodic lattice systems with weak disorder. It is thus an intriguing question to ask: can topological edge floppy modes exist in disordered systems that are completely off lattice?

In this Letter, we study floppy edge modes in disordered fiber networks which are not periodic in space [Figs. 1(b)–1(d)]. Fiber networks are ubiquitous in nature, taking the form of cell cytoskeleton and extracellular matrix, and in man-made materials, taking the form of fiber hydrogels and aerogels, felt, etc., and exhibit fascinating physics [30–41]. Using both analytic theory and numerical simulation, we show that topological edge floppy modes arise in these disordered fiber networks when they are driven away from the simple geometry where all fibers are straight, and these edge floppy modes lead to strongly asymmetric mechanical properties at opposite ends of the fiber network. These topological edge modes may have interesting consequences in a wide range of problems, such as cell cytoskeleton under active driving and the design of smart fiber materials.

Model and results.—We choose the “Mikado model,” which is a completely off lattice 2D fiber network model [30,31], and modify it for our study of topological edge modes. The original Mikado model consists of straight fibers randomly placed on a 2D plane, with all crossing points being free hinges [Fig. 1(b)]. The Hamiltonian of a Mikado model can be written as

$$H = \sum_{i=1}^{N_{\text{fiber}}} \sum_{m=1}^{n_i-1} \frac{k_{i,m}}{2} (|\vec{R}_{i,m} - \vec{R}_{i,m+1}| - \ell_{i,m})^2 + \sum_{i=1}^{N_{\text{fiber}}} \sum_{m=2}^{n_i-1} \frac{\kappa_{i,m}}{2} (\Delta\theta_{i,m})^2, \quad (1)$$

where there are N_{fiber} fibers labeled by i , each has n_i crosslinks labeled by m , and $\vec{R}_{i,m}$ is the (displaced) position of the m th cross-link on the i th fiber. The first term denotes central force stretching energy of each fiber segment (bond)

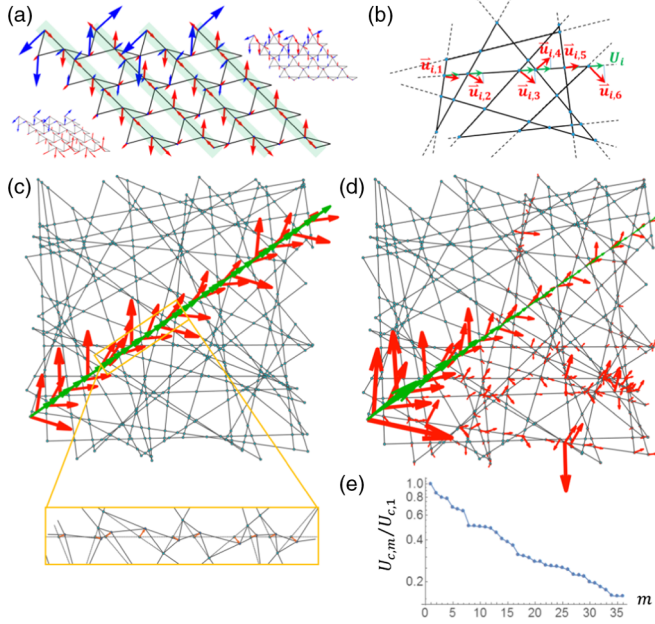


FIG. 1. (a) A deformed kagome lattice in its critical state (middle, large) between two phases with different topologies in their phonon bands (left and right, small). Blue and red arrows show a pair of floppy modes, under periodic boundary condition in the horizontal (x) direction and open boundary condition in the y direction. The pair of floppy modes are on the top and bottom edges, respectively, in the topologically trivial phase (left). The red mode becomes a bulk mode at the transition (middle, where the cyan stripes show the straight lines of bonds) and shift to the top edge in the topological phase (right). (b) An example of an original Mikado network, showing one bulk floppy mode along fiber i (red arrows). This floppy mode is characterized by a constant longitudinal projection of displacements along the fiber U_i (green arrows), and the displacement vectors of the cross-links $\vec{u}_{i,m}$ (red arrows) are perpendicular to the crossing fiber so they are only stretched to second order. Dangling ends are shown as dashed lines and are ignored in the analysis. (c) An example of an original Mikado network, showing the bulk floppy mode on the central fiber which is used to obtain the modified Mikado model (red and green arrows showing $\vec{u}_{c,m}^{(0)}$ and $U_c^{(0)}$, respectively, magnified by 50 times). The enlargement below shows details of the displacements ($\vec{u}_{c,m}^{(0)}$ magnified by 10 times) in a local area [boxed in (a)] that leads to the modified Mikado model. (d) Floppy mode localized on the tail of the central fiber in the modified Mikado model ($\vec{u}_{c,m}^{(0)}$ too small to be visible, red and green arrows denote $\vec{u}_{c,m}$, $U_{c,m}$ of the floppy mode, respectively). (e) Projection of the floppy mode to each segment $U_{c,m}$ [green arrows in (d)] exponentially decrease from tail ($m = 1$) to head ($m = n_c$) on the central fiber.

between neighboring cross-links (sites) m , $m + 1$ along each fiber i , with stretching spring constant $k_{i,m}$ and rest length $\ell_{i,m}$. The second term denotes bending energy of the fiber and $\Delta\theta_{i,m} = \theta_{i,m} - \theta_{i,m-1}$ is the angle change between the two segments meeting at cross-link m along fiber i (here $\theta_{i,m}$ denotes the orientation of the m th segment on fiber i) with bending spring constant $\kappa_{i,m}$.

In typical fiber networks composed of long slender filaments, the bending stiffness is much smaller compared to the stretching stiffness [$\kappa/(k\ell_0^2) \ll 1$ where ℓ_0 is the characteristic mesh size; see discussion in the Supplemental Material [42]]. For our discussion of topological mechanics we first ignore bending stiffness and treat all fiber segments as central-force springs ($\kappa_{i,m} = 0$). Later we use numerical simulations to verify that the essential conclusion of the asymmetric mechanical properties due to edge modes still holds in presence of small bending stiffness.

The original Mikado model displays an interesting property: all floppy modes are *bulk* modes. This can be seen in the following analysis. The total number of cross-links is $N_s = \sum_{i=1}^{N_{\text{fiber}}} n_i/2$ (each cross-link is shared by two fibers) and the total number of bonds is $N_c = \sum_{i=1}^{N_{\text{fiber}}} (n_i - 1)$ (dangling ends are removed since they do not contribute to mechanical stability). The number of zero modes is thus equal to the number of fibers $N_0 = N_s d - N_c = N_{\text{fiber}}$. A straightforward decomposition of the N_{fiber} zero modes is that each fiber carries one zero mode corresponding to the longitudinal displacement of that fiber, while keeping all other fibers intact (the fiber segments crossing the displaced fiber is stretched only to second order in the mode), as shown in Fig. 1(b) [34].

The original Mikado network can be seen as a disordered analog of the critical state of the deformed kagome lattice, in the sense that they both have straight filaments which carry bulk floppy modes [Figs. 1(a)–1(b)]. The deformed kagome lattice exhibits phases (related by a soft strain from the critical state) with different topologies where the floppy modes localize at different edges. Can the Mikado network also exhibit such topological transitions? The answer is yes.

Because what drives the topological transition and the localization of the floppy modes in the deformed kagome lattice is the change of lattice geometry (induced by the soft strain equivalent to the $\vec{q} = 0$ bulk floppy mode), it is natural to consider following bulk floppy modes the original Mikado model and examine their effect on mode localization. As shown in Fig. 1(c), we perturb the Mikado model to create a new ground state as follows: one arbitrarily chosen “central fiber,” c is longitudinally displaced by a small amount $U_c^{(0)}$ [each cross-link on this fiber displaced by $\vec{u}_{c,m}^{(0)} = U_c^{(0)} \{[\sin(\theta_c + \Theta_{c,m})]/[\sin \Theta_{c,m}], -[\cos(\theta_c + \Theta_{c,m})]/[\sin \Theta_{c,m}]\}$, where θ_c is the angle of the central fiber, and $\Theta_{c,m}$ is the intersecting angle between the crossing fiber at cross-link m and the central fiber] following one floppy mode of the original Mikado model. We choose the convention that if the fiber is pulled in the direction pointing from cross-link 1 to n_c on the central fiber (so cross-link n_c is the “head” of motion), $U_c^{(0)} > 0$, and vice versa, and we ignore the resulting stress (which is second order in $U_c^{(0)}$). This geometric perturbation leads us to a new model which we name the “modified Mikado model.”

We then study mechanical properties of the modified Mikado model using both analytical and numerical calculations. The analytic method we adopt to study the modified Mikado network is based on a transfer matrix that propagates floppy modes through cross-links in the network. Transfer matrix methods have been broadly used in various fields, including wave propagation, quantum mechanics, and statistical mechanics to solve problems by decomposing systems into layers of lower dimensions. The way we apply the transfer matrix on the Mikado network is similar as in Ref. [25] with the important difference that in Ref. [25] floppy modes propagate through rows of a periodic lattice, whereas here floppy modes are propagated through individual cross-links in the disordered network.

When a fiber is not straight, floppy modes longitudinal projection is different from segment to segment in the modified Mikado model. Relating floppy-mode displacement of each cross-link $\{\vec{u}_{i,m}\}$ to its longitudinal projection on each fiber segment $\{U_{i,m}\}$, we obtain an equation at each cross-link [Fig. 2(a)]

$$M \begin{pmatrix} U_{i,m-1} \\ U_{j,n-1} \end{pmatrix} = \begin{pmatrix} U_{i,m} \\ U_{j,n} \end{pmatrix}, \quad (2)$$

with the transfer matrix at this cross-link (which is labeled m th on fiber i and n th on fiber j) is

$$M = \begin{pmatrix} \frac{\sin(\Theta_{i,m} - \Delta\theta_{i,m})}{\sin \Theta_{i,m}} & \frac{\sin \Delta\theta_{i,m}}{\sin \Theta_{i,m}} \\ -\frac{\sin \Delta\theta_{i,n}}{\sin \Theta_{i,m}} & \frac{\sin(\Theta_{i,m} + \Delta\theta_{j,n})}{\sin \Theta_{i,m}} \end{pmatrix}, \quad (3)$$

where $\Theta_{i,m} \equiv \theta_{j,n-1} - \theta_{i,m-1}$. This equation serves as a ‘‘transfer matrix’’ for segment displacements at cross-links for an arbitrary floppy mode in the modified Mikado model. For any input of boundary condition in terms of segment displacements on one end of each fiber (remember $N_0 = N_{\text{fiber}}$), we can calculate the floppy mode displacements throughout the whole network.

With this transfer matrix, we can study general floppy modes in the modified Mikado model. We are particularly interested in what happens to the floppy mode that was a bulk mode on the central fiber in the original Mikado model [Figs. 1(b), 1(c)]. To do this, we take the boundary condition that the first segment of every fiber is given to be $U_{i,1} = 0$ if $i \neq c$ and $U_{i,1} = U$ if $i = c$; i.e., only the central fiber has a longitudinal displacement input at segment 1, while all other fibers are held fixed at their segment 1. We then use the transfer matrix [Eq. (2)] to calculate the floppy displacement on the rest of the network. Figure 1(d) shows an example of such an exact calculation, where the resulting floppy mode becomes localized at the tail of the central fiber.

To characterize such floppy mode localization we take the following perturbative expansion. Because fibers in the modified Mikado model are close to straight ($U_c^{(0)}$ is small), all $\Delta\theta_{i,m}$ are small, which permits a perturbative expansion

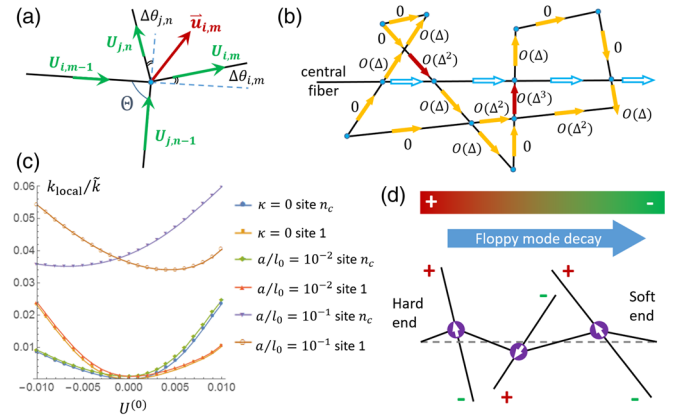


FIG. 2. (a) Illustration of the transfer matrix [Eq. (3)] applying on a cross-link. (b) Displacements propagation (along arrows) and order of magnitude when applying the transfer matrix on the network with boundary condition that only cross-link 1 of the central fiber has input U (large blue arrows for $O(1)$, smaller arrows for higher order in Δ and red denotes flow back to the central fiber). (c) Asymmetric edge stiffness at two ends of the central fiber. We perform numerical simulations to measure local stiffness k_{local} against point force on two ends of the central fiber, in modified Mikado models with different $U^{(0)}$. We show results for both networks with no bending stiffness $\kappa = 0$ and with bending stiffness (controlled by fiber thickness a in unit of characteristic mesh size ℓ_0 , and we normalize k_{local} using characteristic spring constant of one segment \tilde{k}). For more details see the Supplemental Material [42]. In all cases, the head is significantly more stiff than the tail. (d) Mikado network under active driving from active cross-links (marked with arrows) on the central fiber. The direction of driving is determined by the chirality of the crossing fibers, such that the motors actively move to the ‘‘+’’ end. If all crossing fibers have correlated chirality such that their + ends are on the left, from Eq. (4), we find that the floppy mode on the central fiber exponentially localizes to the left.

of the transfer matrix at small bending angles (represented generally by Δ) and allows further analysis. Following the central fiber, we find that at each cross-link (for more details see the Supplemental Material [42]),

$$U_{c,m} = [1 - \Delta\theta_{c,m} \cot \Theta_{c,m} + \mathcal{O}(\Delta\theta_{c,m}^2)] U_{c,m-1}, \quad (4)$$

where we have used the fact that the input $U_{j,n-1}$ from the fiber that crosses the central fiber is either 0 (from boundary condition), or of $\mathcal{O}(\Delta^2)$ or higher (from other cross-links on the central fiber itself through a loop), as shown in Fig. 2(b). Such higher-order displacements are visible in Fig. 1(c) where we used the full transfer matrix [Eq. (3)]. This small Δ expansion also requires that the crossing angles $\Theta_{c,m}$ are not too small (so $\cot \Theta_{c,m}$ does not diverge), a condition naturally satisfied in most fiber networks from excluded volume repulsion.

Equation (4) governs the growth and decay of the floppy mode along the central fiber. If $\cot \Theta > 0$, we have $U_{c,m} > (<) U_{c,m-1}$ if $\Delta\theta_{i,m} < (>) 0$ [corresponding to the central

fiber bending up (down) at this cross-link], and vice versa (see Supplemental Material [42] for examples of the geometry). This is a very general geometric rule for edge floppy modes, which applies to the case of topological kagome lattices as well [e.g., following the two families of vertical lines up in Fig. 1(c) one finds that U increases on both]. This rule can also be used to design new ordered or disordered structures which exhibit tailored distribution of floppy modes (see example in the Supplemental Material [42]). The advantage of designs based on disordered structures, compared to existing designs of periodic topological mechanical metamaterials, is that they may be easier to implement in systems such as foams and aerogels where one just need to introduce certain asymmetry in the disordered structure to obtain floppy edge modes, without the need to precisely control the structure to ensure periodicity.

Now with the general rule of floppy mode evolution at each cross-link, we come back to the question of where the floppy mode localizes in the modified Mikado model. It is straightforward to see that individually at each cross-link (holding all other crosslinks fixed) the displacement $U_{c,m}^{(0)}$ points to the direction of floppy mode $U_{c,m}$ decreasing along the central fiber if $U_c^{(0)} > 0$ (central fiber pulled towards cross-link n_c), and vice versa. However, we need to rigorously prove that in the modified Mikado model where all crosslinks are displaced along the central fiber at the same time, the disorder averaged (denoted by $\langle \dots \rangle$) decay rate of the floppy mode

$$\langle \lambda \rangle \equiv 1 - \left\langle \frac{U_{c,m+1}}{U_{c,m}} \right\rangle \quad (5)$$

is positive when $U_c^{(0)} > 0$ and negative when $U_c^{(0)} < 0$ (floppy mode localizes on tail), given the condition that different fibers have uncorrelated orientations. The proof is included in the Supplemental Material [42].

The analytic theory discussed above is at zero bending stiffness, but our numerical results show that when bending stiffness is introduced, the asymmetric stiffness is still significant [Fig. 2(c)].

The floppy edge modes we find in these disordered fiber networks are of the same geometric origin as topological edge floppy modes in periodic lattices. In discussions above we constructed a real space transfer matrix method that shows the exponential localization of floppy modes on individual fibers. Next we show that a topological invariant, a generalization of the ‘‘topological polarization’’ defined in Ref. [2] to disordered networks, can be defined on the central fiber that dictates its edge floppy mode. In order to do this we start by introducing the compatibility matrix $C_{\beta m}$ which maps site displacements (projected to bond m) $U_{c,m}$ onto bond extensions $\delta l_{c,\beta}$

$$\delta l_{c,\beta} = \sum_{m=1}^{n_c} C_{\beta m} U_{c,m}, \quad (6)$$

where the subscript c refers to central fiber, and subscripts β, m label the bonds and the sites, respectively. The form of $C_{\beta m}$ is determined by the transfer matrix, as detailed in the Supplemental Material [42]. We then rewrite this equation in momentum space, where the compatibility matrix takes the form $\tilde{C}(q_1, q_2)$, where q_1, q_2 are momenta corresponding to real space variables β, m , respectively (note that \tilde{C} depends on two momenta as a result of disorder instead of one in the periodic lattice case). Existence of floppy modes is determined by the equation $\det \tilde{C} = 0$ which generally has no solution under periodic boundary condition. Edge floppy modes under an open boundary condition is captured by introducing an extra complex component to the momenta, $k = k' + ik''$ (note the same k is added to both q_1, q_2 because they are in the same dimension). The sign of k'' , which governs which end of the fiber the floppy mode localizes to, is determined by a topological invariant, the winding number

$$\mathcal{N}_c = \frac{1}{n_c} \frac{1}{2\pi} \oint_0^{2\pi} dk \frac{d}{dk} \text{Im} \ln \det \tilde{C}(q_1 + k, q_2 + k), \quad (7)$$

such that $\mathcal{N}_c = 0, 1$ correspond to the floppy mode on the right and left, respectively. The actual solution k'' is directly related to the decay rate λ on the fiber. Different network geometries having the same \mathcal{N}_c for a given central fiber are related to one another by continuous deformations without closing the bulk gap of that fiber. An expanded discussion of \mathcal{N}_c is in the Supplemental Material [42].

Discussions.—In this Letter we show that in disordered fiber networks, when individual fibers are pulled, a topological edge floppy mode localizes on the tail of the fiber. Now we generalize this conclusion and discuss possible application to experimental systems.

First, the scenario of pulling fibers in a network occurs in various situations. For example, myosin motors exert active pulling stress on actin filaments and are a main source of activity in the cytoskeleton. Another example is the active pulling by tumor cells on the extracellular matrix when they invade into surrounding tissue. It would be interesting to explore the biological consequences of edge floppy modes that may arise as a result of such pulling. Our discussions above focus on 2D fiber networks and thus directly apply to 2D networks such as the actomyosin cortex that encloses cells and the nuclear lamina that encloses cell nucleus. Analogous floppy edge modes in 3D fiber networks will be the next step of study and may have more interesting consequences. In addition, although our discussions specialize to the case of one single fiber being pulled, in the Supplemental Material [42], we include numerical results for networks in which multiple fibers are pulled simultaneously, where we show edge floppy modes on each pulled fiber, as well as how macroscopic deformations can also generate asymmetric edge stiffness due to these edge modes. Moreover, in the modified Mikado network we

ignored the (higher order) stress generated in the ground state. Including these residual stresses only shifts the equilibrium force of the head and the tail of the fibers, and the asymmetric stiffness remains true (see Supplemental Material [42] for more discussion).

Second, although our discussion is based on the simple geometric perturbation that one central fiber is pulled, the transfer matrix method we develop applies to the more general situation of geometric perturbation of the fiber network, because the exponential increase or decrease of the floppy mode only depends on the relation between the crossing fiber orientation and the direction of bending of the central fiber. This type of change of geometry in fiber networks can occur in a rich variety of systems. For example, in a network where some or all of the cross-links are active motors that walk on particular directions on the fibers [43–45], such coherent change in geometry can also happen. As shown in Fig. 2(d), where a central fiber is cross-linked to other fibers via active motors, and the chirality of the crossing fibers are correlated, a topological edge floppy mode emerges on the central fiber due to the active driving.

This work was supported by the National Science Foundation Grant No. NSF DMR-1609051.

-
- [1] E. Prodan and C. Prodan, *Phys. Rev. Lett.* **103**, 248101 (2009).
- [2] C. L. Kane and T. C. Lubensky, *Nat. Phys.* **10**, 39 (2014).
- [3] T. C. Lubensky, C. Kane, X. Mao, A. Souslov, and K. Sun, *Rep. Prog. Phys.* **78**, 073901 (2015).
- [4] P. Wang, L. Lu, and K. Bertoldi, *Phys. Rev. Lett.* **115**, 104302 (2015).
- [5] L. M. Nash, D. Kleckner, A. Read, V. Vitelli, A. M. Turner, and W. T. Irvine, *Proceedings of the National Academy of Sciences* **112**, 14495 (2015).
- [6] R. Süsstrunk and S. D. Huber, *Science* **349**, 47 (2015).
- [7] S. H. Mousavi, A. B. Khanikaev, and Z. Wang, *Nat. Commun.* **6**, 8682 (2015).
- [8] Z. Yang, F. Gao, X. Shi, X. Lin, Z. Gao, Y. Chong, and B. Zhang, *Phys. Rev. Lett.* **114**, 114301 (2015).
- [9] V. Peano, C. Brendel, M. Schmidt, and F. Marquardt, *Phys. Rev. X* **5**, 031011 (2015).
- [10] C. Stroh, G. L. J. A. Rikken, and P. Wyder, *Phys. Rev. Lett.* **95**, 155901 (2005).
- [11] L. Sheng, D. N. Sheng, and C. S. Ting, *Phys. Rev. Lett.* **96**, 155901 (2006).
- [12] R. K. Pal, M. Schaeffer, and M. Ruzzene, *J. Appl. Phys.* **119**, 084305 (2016).
- [13] C. He, X. Ni, H. Ge, X.-C. Sun, Y.-B. Chen, M.-H. Lu, X.-P. Liu, and Y.-F. Chen, *Nat. Phys.* **12**, 1124 (2016).
- [14] R. Süsstrunk and S. D. Huber, *Proc. Natl. Acad. Sci. U.S.A.* **113**, E4767 (2016).
- [15] M. Xiao, W.-J. Chen, W.-Y. He, and C. Chan, *Nat. Phys.* **11**, 920 (2015).
- [16] D. Z. Rocklin, B. G. G. Chen, M. Falk, V. Vitelli, and T. C. Lubensky, *Phys. Rev. Lett.* **116**, 135503 (2016).
- [17] D. Z. Rocklin, S. Zhou, K. Sun, and X. Mao, *Nat. Commun.* **8**, 14201 (2017).
- [18] J. Paulose, A. S. Meeussen, and V. Vitelli, *Proc. Natl. Acad. Sci. U.S.A.* **112**, 7639 (2015).
- [19] J. Paulose, B. G. -g. Chen, and V. Vitelli, *Nat. Phys.* **11**, 153 (2015).
- [20] B. G. -g. Chen, N. Upadhyaya, and V. Vitelli, *Proceedings of the National Academy of Sciences* **111**, 13004 (2014).
- [21] A. Souslov, A. J. Liu, and T. C. Lubensky, *Phys. Rev. Lett.* **103**, 205503 (2009).
- [22] X. Mao, N. Xu, and T. C. Lubensky, *Phys. Rev. Lett.* **104**, 085504 (2010).
- [23] W. G. Ellenbroek and X. Mao, *Europhys. Lett.* **96**, 54002 (2011).
- [24] X. Mao and T. C. Lubensky, *Phys. Rev. E* **83**, 011111 (2011).
- [25] K. Sun, A. Souslov, X. Mao, and T. C. Lubensky, *Proc. Natl. Acad. Sci. U.S.A.* **109**, 12369 (2012).
- [26] L. Zhang, D. Z. Rocklin, B. G. G. Chen, and X. Mao, *Phys. Rev. E* **91**, 032124 (2015).
- [27] X. Mao, A. Souslov, C. I. Mendoza, and T. C. Lubensky, *Nat. Commun.* **6**, 5968 (2015).
- [28] D. M. Sussman, O. Stenull, and T. Lubensky, *Soft Matter* **12**, 6079 (2016).
- [29] N. P. Mitchell, L. M. Nash, D. Hexner, A. Turner, and W. Irvine, [arXiv:1612.09267](https://arxiv.org/abs/1612.09267).
- [30] D. A. Head, A. J. Levine, and F. C. MacKintosh, *Phys. Rev. Lett.* **91**, 108102 (2003).
- [31] J. Wilhelm and E. Frey, *Phys. Rev. Lett.* **91**, 108103 (2003).
- [32] M. Gardel, J. Shin, F. MacKintosh, L. Mahadevan, P. Matsudaira, and D. Weitz, *Science* **304**, 1301 (2004).
- [33] C. Storm, J. Pastore, F. MacKintosh, T. Lubensky, and P. Janmey, *Nature (London)* **435**, 191 (2005).
- [34] C. Heussinger and E. Frey, *Phys. Rev. Lett.* **97**, 105501 (2006).
- [35] C. P. Broedersz, X. Mao, T. C. Lubensky, and F. C. MacKintosh, *Nat. Phys.* **7**, 983 (2011).
- [36] X. Mao, O. Stenull, and T. C. Lubensky, *Phys. Rev. E* **87**, 042601 (2013).
- [37] X. Mao, O. Stenull, and T. C. Lubensky, *Phys. Rev. E* **87**, 042602 (2013).
- [38] C. P. Broedersz and F. C. MacKintosh, *Rev. Mod. Phys.* **86**, 995 (2014).
- [39] A. Sharma, A. Licup, K. Jansen, R. Rens, M. Sheinman, G. Koenderink, and F. MacKintosh, *Nat. Phys.* **12**, 584 (2016).
- [40] J. Feng, H. Levine, X. Mao, and L. M. Sander, *Phys. Rev. E* **91**, 042710 (2015).
- [41] J. Feng, H. Levine, X. Mao, and L. M. Sander, *Soft Matter* **12**, 1419 (2016).
- [42] See Supplemental Material at <http://link.aps.org/supplemental/10.1103/PhysRevLett.120.068003> for additional analytic and numerical results.
- [43] B. Alberts, A. Johnson, J. Lewis, M. Raff, K. Roberts, and P. Walter, *Molecular Biology of the Cell*, 4th ed. (Garland, New York, 2008).
- [44] C. P. Brangwynne, G. H. Koenderink, F. C. MacKintosh, and D. A. Weitz, *J. Cell Biol.* **183**, 583 (2008).
- [45] J.-F. Joanny and J. Prost, *HFSP J.* **3**, 94 (2009).